Study of ratchet limit and cyclic response of welded pipe

Manu Puliyaneth[1], Daniele Barbera[2], Haofeng Chen[1, 3] (✉), Fuzhen Xuan[3]

[1]Department of Mechanical & Aerospace Engineering, University of Strathclyde, Glasgow, G1 1XJ, UK

[2]School of engineering, Systems Power and Energy Division, University of Glasgow, Glasgow, G12 8QQ, UK

[2]School of Mechanical & Power Engineering, East China University of Science & Technology, Shanghai 200237, China

Abstract Ratcheting and low cycle fatigue are failure mechanisms observed in components subjected to cyclic temperature and mechanical loads. Ratcheting is a global failure mechanism which leads to an incremental plastic collapse of the component whereas low cycle fatigue is a localized mechanism which leads to crack initiation. It is exacerbated by grooves, notches and changes in the geometry of the component. To estimate the remaining life of the component and predict its failure mechanism, it is important to understand how it responds to various combinations of cyclic loads. This paper includes investigation of the ratchet limit and the plastic strain range, which is associated with the low cycle fatigue, of a circumferential butt-welded pipe by using the ratchet analysis method which includes Direct Steady Cycle Analysis (DSCA) within the Linear Matching Method Framework (LMMF). The pipe is subjected to a constant internal pressure and a cyclic thermal load. The investigation is carried out by varying 1) material properties of the weld metal (WM); 2) ratio of inner radius to wall thickness; 3) weld geometry. Within the specified ranges, yield stress and the ratio of inner radius to wall thickness affect the ratchet limit curve. The cyclic thermal load plays a crucial role compared to the internal pressure in influencing the ratchet limit curve. It is observed that the pipe experiences thermal ratcheting in the absence of pressure load at lower yield stress values of the WM. The results obtained are combined to create a limit load envelope, which can be used for the design of welded pipes within the specified ranges.

Keywords Welded Pipe, Linear Matching Method, Ratcheting, Low Cycle Fatigue, Direct Method

1 Introduction

A circumferential butt welded pipe subjected to a cyclic thermal and/or a mechanical load can behave in one of the three manners, namely shakedown, reverse plasticity (plastic shakedown) or ratcheting. The structure is said to be under elastic shakedown when an elastic response is obtained after the first few load cycles [1]. Beyond the elastic shakedown limit, the body exhibits either plastic shakedown or

E-mail: haofeng.chen@strath.ac.uk
Tel: +44 (0) 1415 482 036
Homepage(optional): thelmm.co.uk

ratcheting. In certain cases, it is acceptable for the body to be under plastic shakedown as long as the low cycle fatigue that occurs during this phase is also considered during the design phase[1] whereas a structure under ratcheting is generally avoided unless if both the number of cycles and the ratchet strain per cycle is small. A body is considered to be ratcheting when the plastic strain increases with each cycle, which eventually leads to the structural failure mechanism [2]. In the literature, a significant amount of effort has been dedicated in understanding the cyclic response of different components subjected to cyclic loading [3]–[5].

Ratcheting can be studied and discussed in two aspects, structural ratcheting and material ratcheting [6], [7]. Structural engineers associate ratcheting as a phenomenon where the strain increases by a constant amount in each load cycle whereas engineers from the material research domain associate ratcheting as an accumulation of strain even if gradually the rate of accumulation decreases and a steady state is reached [7]. Material ratcheting is a material related effect and hardening of the material plays an important role. Structural ratcheting can occur even in the absence of material ratcheting. For structural ratcheting, whether or not a ratcheting mechanism is prevalent in a structure of a particular geometry and loading can be illustrated using a ratcheting interaction diagram. The ratcheting interaction diagrams are generally constructed based on a constant primary stress and a cyclic secondary stress. Once the ratcheting interaction diagram is developed for the specific geometry and loading condition, they can be used to determine whether the considered set of loading conditions will lead to excessive strain accumulation thereby leading to ratcheting. With the elastic-perfectly plastic (EPP) model, strain accumulates infinitely within the region R (as indicated in Fig. 2), on the other hand, if hardening is introduced then plastic shakedown may occur after a number of cycles such that strain accumulation is bounded. This state is referred to as finite ratcheting in material ratcheting. Material ratcheting is simulated by taking the cyclic stress-strain results and using them in an appropriate hardening plasticity model such as Frederick-Armstrong [8] model and Chaboche model [9]–[11]. In this study, only structural ratcheting is considered, hence the word “ratcheting” or ‘’ratchet’’ refers to structural ratcheting only.

Due to the complexity of obtaining analytical solutions for reverse plasticity or ratcheting limit analysis, Finite Element Analysis (FEA) is used to address such challenges. A limitation in using incremental FEA analysis is that it can only predict how the structure will behave under the chosen set of load points, i.e. whether the body will exhibit shakedown behaviour or ratcheting behaviour [12]. The aforementioned strategy does not allow to determine easily the more comprehensive interaction diagrams such as the Bree-diagram, which accounts for several cyclic load combinations. In order to overcome this problem many direct methods, such as 1) Uniform Modified Yield (UMY) surface method [13]; 2) The Elastic Compensation method (ECM)[14]; 3) the Generalized Local Stress-Strain r-node method [15]; 4) the Linear Matching Method (LMM) have been formulated which uses simple material models like the elastic-perfectly plastic model. They are generally based on Koiter’s kinematic [16] and/or Melan’s static theorems. Direct methods don’t require the knowledge of the exact load path as they consider a loading domain that contains all possible path between the extreme load points [1].

Welded pipes are widely used in many industries and they are usually exposed to both cyclic thermal and mechanical loads. It has been of interest to study the variations in the reverse plasticity and

ratchet limits of welded pipes. This is because welds are sites of geometric irregularities, in the form of joint configurations or weld profile which leads to local stress concentration that affect the fatigue life of the pipe[17]. This paper aims at performing a ratchet limit-parametric study along with cyclic response assessment of a butt welded pipe subjected to a constant internal pressure and a cyclic thermal load by using LMM. The validity of LMM for ratcheting analysis has been proved in [6, 11, 12]. This paper consists of six sections. Section 2 provides a brief introduction to the linear matching methodology used for the analysis. Section 3 presents the pipe geometry, material properties and FE model. Section 4 presents the ratchet analysis and cyclic response assessment study of the baseline model considered and the results of the parametric study done by varying 1) material properties of the WM; 2) ratio of inner radius to wall thickness; 3) weld geometry. Section 5 presents further discussions. Finally, section 6 includes the conclusions of this study.

2 Linear Matching Method (LMM)

The theoretical ground for LMM is that the nonlinear elastic behaviour of a structure can be mimicked by a series of linear elastic solutions where the moduli vary spatially and with time [20]. The evolution of LMM in determining the limit-loads, the shakedown limits, the plastic strain range and the ratchet limits have been previously described in [15, 12, 14, 16, 17]. Hence, only a concise version of the numerical procedure is presented in this section.

Consider an elastic-perfectly plastic body of volume, V and surface area, S. It is subjected to a general cyclic load history, F (x_i, t), that can be decomposed to a cyclic temperature history θ (x_i, t) which acts within the volume, a varying mechanical load P(x_i, t) and a constant mechanical load, $\overline{F}$ (x_i). The loads act over a time cycle of $0 \le t \le \Delta t$.

$$F(x_i, t)=\lambda \overline{F}(x_i)+\theta(x_i, t)+P(x_i, t) \tag{1}$$

where λ is the load parameter. The corresponding linear elastic stress history is given by:

$$\hat{\sigma}_{ij}(x_k,t) = \lambda\hat{\sigma}_{ij}^{\overline{F}} + \lambda\hat{\sigma}_{ij}^{\Delta}(x_k,t) \text{ where } \hat{\sigma}_{ij}^{\Delta} = \hat{\sigma}_{ij}^{P} + \hat{\sigma}_{ij}^{\theta} \tag{2}$$

where $\hat{\sigma}_{ij}^{\overline{F}}$, $\hat{\sigma}_{ij}^{P}$ and $\hat{\sigma}_{ij}^{\theta}$ represent the elastic stresses due to $\overline{F}$ (x_i), P (x_i, t) and θ (x_i, t) respectively. The load parameter λ allows a range of loading histories to be considered. Stress and strain rates asymptotes to a cyclic state where

$$\sigma_{ij}(t) = \sigma_{ij}(t+\Delta t) \qquad \dot{\varepsilon}_{ij}(t) = \dot{\varepsilon}_{ij}(t+\Delta t) \tag{3}$$

Equation 4 is the general stress solution for the cyclic problem defined. $\overline{\rho}_{ij}$ is the constant residual stress field in equilibrium with zero surface traction and denotes the residual stress at the beginning and end of the cycle.

$$\sigma_{ij}(x_k,t) = \hat{\sigma}_{ij}(x_k,t) + \overline{\rho}_{ij}(x_k) + \rho_{ij}^{r}(x_k,t) \tag{4}$$

ρ_{ij}^{r} is the change in residual stress during the cycle and satisfies

$$\rho_{ij}^{r}(x_k,0) = \rho_{ij}^{r}(x_k,\Delta t) = 0 \tag{5}$$

In order to address the ratchet limit analysis, we decouple the evaluation of the changing residual stress $\rho_{ij}^{r}(t)$ due to the cyclic part of the load and the constant residual stress $\overline{\rho}_{ij}^{\overline{F}}$. The varying and constant parts of the residual stresses are evaluated separately. Ratchet limit analysis using LMM consists of two steps. The first step involves an incremental minimization for the evaluation of the cyclic history of residual stress and the plastic strain range, this step calculates the history of residual stress field related to the cyclic load and the corresponding plastic strain ranges associated with the low cycle fatigue assessment. The second step involves a global minimization for the ratchet limit due to an extra constant load, this step locates the ratchet limit as a conventional shakedown limit where a constant residual stress is evaluated and the elastic stress history is augmented by the changes in the residual stress calculated in the first step.

2.1 Numerical procedure for plastic strain range

The residual stress history and the plastic strain due to the cyclic component of the load history are expressed in terms of N discrete time points in the LMM numerical procedure. For a strictly convex yield condition, the instants when plastic strains occur are at the vertices of the stress history, $\hat{\sigma}_{ij}^{\Delta}(t_n)$ n=1 to N, where N represents the total number of time instants, t_1, t_2, t_3....t_N. Then $\Delta\varepsilon_{ij}^{T} = \sum_{n=1}^{N}\Delta\varepsilon_{ij}^{P}(t_n)$ is the plastic strain accumulated during the cycles; $\Delta\varepsilon_{ij}^{P}$ defines the increment of plastic strain at t_n. We also define $\Delta\rho_{ij}{}_{m}^{n}$ as the evaluated changing residual stress for the n^{th} load instance at the m^{th} cycle of integration; n=1 to N and m=1 to M. The iteration process starts with the first increment where $\Delta\rho_{ij}{}_{1}^{1}$ is solved, due to the elastic solution at first load instance. At the next increment, $\Delta\rho_{ij}{}_{1}^{2}$ is solved, which is due to the previously calculated residual stress and the elastic stress at second load instance. The incremental iterative process continues until convergence is achieved i.e. $\sum_{n=1}^{N}\Delta\rho_{ij}{}_{M}^{n} = 0$.

The constant element of the residual stress is

$$\rho_{ij}^{r}(0) = \rho_{ij}^{r}(\Delta t) = \overline{\rho}_{ij} \tag{6}$$

where

$$\overline{\rho}_{ij} = \sum_{n=1}^{N}\Delta\rho_{ij}{}_{1}^{n} + \sum_{n=1}^{N}\Delta\rho_{ij}{}_{2}^{n} + \ldots + \sum_{n=1}^{N}\Delta\rho_{ij}{}_{M-1}^{n} \tag{7}$$

Equation 8 gives the converged increment of the plastic strain at t_n

$$\Delta\varepsilon_{ij}^{p}(t_n) = \frac{1}{2\overline{\mu}_n}[\overline{\sigma}_{ij}^{\Delta'}(t_n) + \rho_{ij}^{'}(t_n)] \tag{8}$$

Where $\bar{\mu}_n$ is the iterative shear modulus and $'$ indicates the deviator component of $\bar{\sigma}_{ij}^{\Delta}$ and ρ_{ij}. In order to calculate the ratcheting limit using LMM, we require the history of residual stress field, $\rho_{ij}(t_n)$

$$\rho_{ij}(t_n) = \bar{\rho}_{ij} + \sum_{k=1}^{n} \Delta\rho_{ij}{}_M^k \tag{9}$$

2.2 Numerical procedure for ratchet limit

As indicated in section 2, ratchet limit analysis within the LMM involves two steps. Step one concludes with the determination of $\rho_{ij}(t_n)$. Once this is done, ratchet limit is calculated using the existing shakedown methodology where the predefined linear elastic solution is augmented by the varying residual stress field $\rho_{ij}(t_n)$.

The upper bound limit is based on Koiter's theorem and is given as:

$$\lambda_{UB} = \frac{\int_V \sum_{n=1}^{N} \sigma_y \bar{\varepsilon}\left(\Delta\varepsilon_{ij}^n\right) dV - \int_V \sum_{n=1}^{N} (\hat{\sigma}_{ij}^{\Delta}(t_n) + \rho_{ij}(t_n)) \Delta\varepsilon_{ij}^n dV}{\int_V \hat{\sigma}_{ij}^{\bar{F}} \sum_{n=1}^{N} \left(\Delta\varepsilon_{ij}^n\right) dV} \tag{10}$$

where

$$\bar{\varepsilon}\left(\Delta\varepsilon_{ij}^n\right) = \sqrt{\tfrac{2}{3} \Delta\varepsilon_{ij}^n \Delta\varepsilon_{ij}^n} \tag{11}$$

σ_y is the von Mises yield stress, $\rho_{ij}(t_n)$ is the residual stress at time t_n. $\Delta\varepsilon_{ij}^n$ is the increment of plastic strain that occurs at t_n. λ_{UB} denotes the extra constant load $\hat{\sigma}_{ij}^{\bar{F}}$ the body can endure along with a predefined cyclic load $\hat{\sigma}_{ij}^{\Delta}(t_n)$ before it starts ratcheting. For the fixed displacement filed, LMM then produces a sequence of monotonically reducing upper bounds that converges to the least upper bound ratchet limit.

3 Pipe geometry and material properties and Finite Element Model

The pipe geometry considered is a circumferential welded pipe, which includes a single V butt weld with V root. It is subjected to a constant internal pressure and a cyclic thermal load. The weldment comprises of three zones; 1) the Parent Material (PM), 2) the Weld Material (WM) and 3) Heat Affected Zone (HAZ). It is assumed that all the three zones exhibit elastic-perfectly plastic material properties and that they satisfy the Von Mises yield condition. The residual stress in the pipe due to welding is considered to be zero due to the post weld heat treatment. Pipe geometry is shown in Fig. 1(a) and their dimensions are presented in Table 1. The yield stress is considered to be temperature dependent. Material properties for baseline calculations are indicated in Table 2 [19,20]. The values for k and ν are considered to be the same for all three zones. Due to the limited availability of material properties for HAZ, they are assumed to be the average of PM and WM for this study.

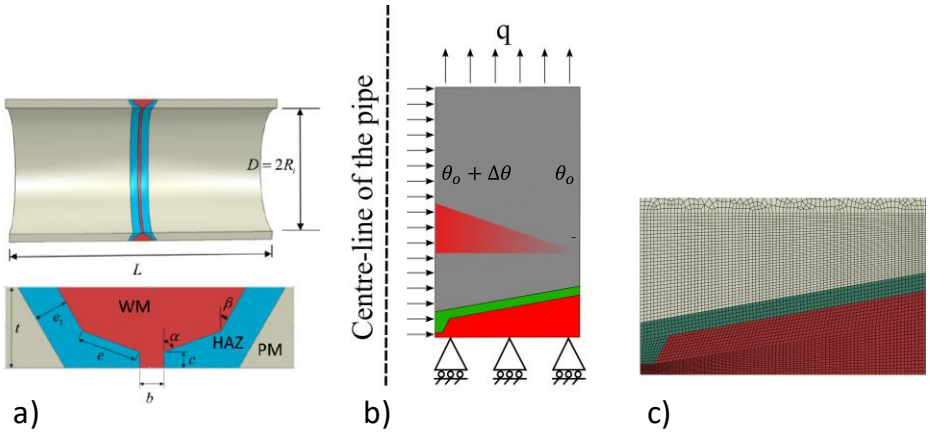

Fig. 1 a) Butt welded pipe geometry with principal geometrical parameters. b) Boundary condition and the load applied to the welded pipe; c) Mesh used for finite element analysis

Table 1 Pipe dimensions

L (mm)	R_i (mm)	t (mm)	e1 (mm)	e (mm)	b (mm)	c (mm)	α (°)	β (°)
1000	300	40	2.5	4.5	3	2	63	10

Table 2 Material properties

E_y^{PM} (GPa)	E_y^{HAZ} (GPa)	E_y^{WM} (GPa)	α^{PM} (x 10-5 °C^{-1})	α^{HAZ} (x 10-5 °C^{-1})	α^{WM} (x 10-5 °C^{-1})	k (Wm^{-1} °C^{-1})	ν
200	220	240	3.8	3.7	3.6	15	0.3

	≤ 20 °C	200 °C	400 °C	600 °C
σ_y^{PM} (MPa)	230	184	132	105
σ_y^{HAZ} (MPa)	345	275.5	198	157
σ_y^{WM} (MPa)	460	367	264	209

An axisymmetric model is used for the analysis, as shown in Fig. 1(b), with symmetric condition applied in the axial direction. The end of pipe is constrained to remain in plane thereby simulating expansion of the pipe. An axial tension (Equation 12) is applied to simulate closed end condition of the pipe.

$$q = \frac{pR_i^2}{2R_i t + t^2} \tag{12}$$

It is assumed that the outside temperature of the pipe is θ_o, and the operating temperature of the fluid in the pipe varies between the outer temperature and a higher value, $\theta_o+\Delta\theta$. The applied cyclic thermal loading can be constructed by three thermal stress extremes: i) a thermal stress field produced by a linear temperature gradient through the wall thickness; ii) a thermal stress field occurring at the highest uniform temperature due to the different thermal expansion coefficients and Young's modulus

between the PM, HAZ and WM; and iii) a zero thermal stress field simulating a uniform ambient temperature. Considering θ_o equal to zero, the maximum effective elastic thermal stresses for the three extremes can be determined by the maximum temperature difference $\Delta\theta$. Hence the thermal load history can be characterised by $\Delta\theta$.

CAX8R 8-node biquadratic axisymmetric quadrilateral elements with reduced integration are used for structural analysis and DCAX8 8-node quadratic axisymmetric heat transfer quadrilateral elements with reduced integration are used for the heat transfer analysis.

4 Results and discussion

The parametric study is conducted to investigate the effects of 1) material properties such as the coefficient of thermal expansion of WM (α^{WM}), Young's modulus of WM (E^{WM}), yield stress of WM (σ_y^{WM}); 2) weld geometry; and 3) ratio of inner radius to wall thickness on the ratchet limit and the plastic strain range.

The plots used for the ratchet limit discussions have a normalised internal pressure, p/p_o and a normalised temperature range, $\Delta\theta/\Delta\theta_o$ as their ordinate and abscissa. p_o = 23 MPa and $\Delta\theta_o$ = 50 °C are the reference internal pressure and cyclic temperature range respectively.

Fig. 2 shows a typical shakedown and ratchet limit interaction curve for the baseline model considered in this study. S, stands for the shakedown region, P indicates reverse plasticity region and R is the ratcheting region. Fatigue analysis is done for two pressure references, p/p_o = 0 (only cyclic temperature load) and p/p_o = 0.25. This is selected as for most cases analysed, they are well within the P region, and provide grounds for better comparison. The load points for plastic strain range analysis are indicated in Fig. 2

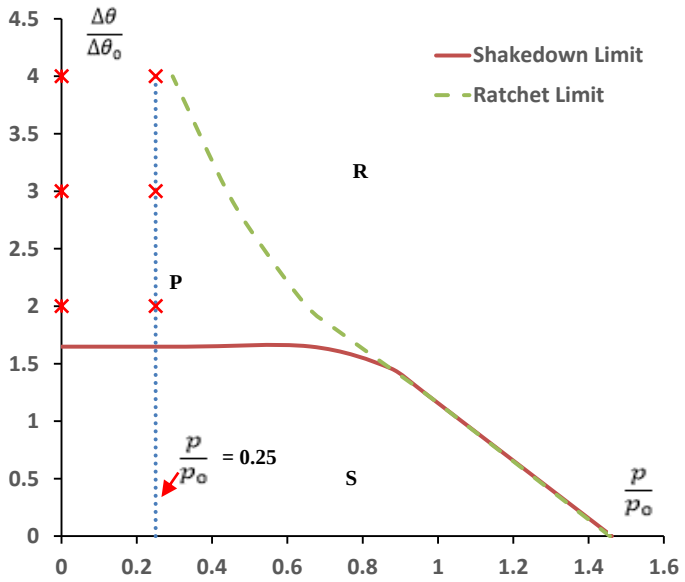

Fig. 2 Load points adopted for fatigue analysis

4.1 Influence of Material properties of weld metal

4.1.1 Effect of Coefficient of Thermal Expansion of weld metal, α^{WM}

In increments of 0.2 x 10^{-5}, α^{WM} is increased from 3.2 x 10^{-5} to 4.6 x 10^{-5}. Fig. 3 shows the ratchet limit curve of the welded pipe for varying values of α^{WM}, it can be seen that they exhibit a typical Bree-like diagram. As ratcheting is a global mechanism, the coefficient of thermal expansion, which only has a localised effect, doesn't affect the ratchet limit.

Fig. 4 indicates the variation of plastic strain range with increasing α^{WM}. It can be observed that the presence of additional mechanical load has only a minimum effect of the plastic strain range. At lower cyclic temperature load, the presence of mechanical load has no effect on the plastic strain range values, whereas at higher cyclic temperature loads a slight increase in the plastic strain range is observed. The plastic strain range decreases to a minimum value as the coefficient of thermal expansion of the weld metal is increased after which it remains constant with and without the presence of additional mechanical load. In all cases analysed the plastic strain range values were maximum at the PM-HAZ interface towards the inner side of the pipe. Also, it should be noted that for the same miss-match factor the plastic strain range is greater at higher temperatures.

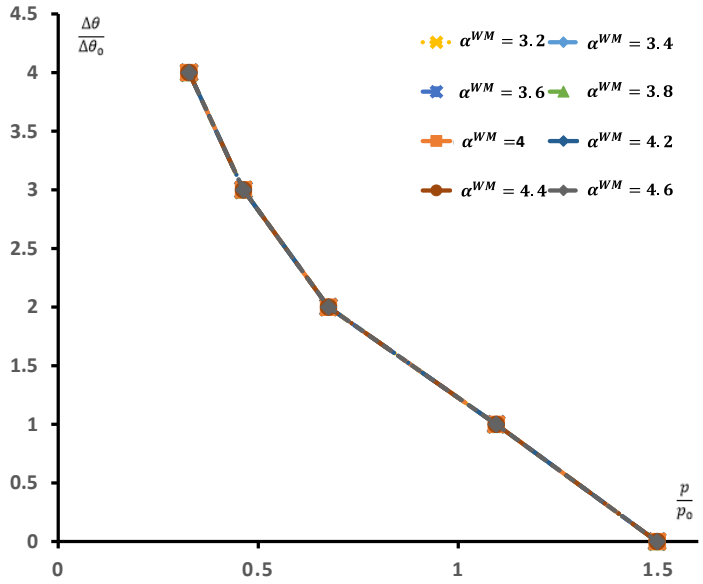

Fig. 3 Ratcheting curves of the welded pipe for varying coefficient of thermal expansion of weld metal

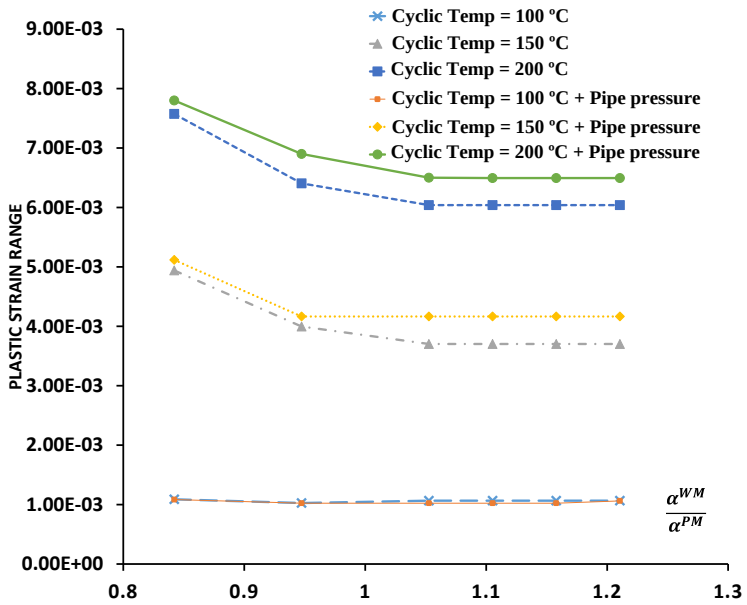

Fig. 4 Comparison of plastic strain range for varying coefficient of thermal expansion of weld metal, with and without mechanical load

4.1.2 Effect of Young's Modulus of weld metal, E^{WM}

Young's modulus of the weld metal, E^{WM} is varied from 80 GPa to 560 GPa, in increments of 80 GPa. Fig. 5 shows the ratchet limit curves obtained, they are congruent and exhibit Bree-like diagram. As reflected in Fig. 5, the Young's modulus of the weld metal does not influence the ratcheting curve or the limit load. This is because, as mentioned in the previous subsection, ratcheting is a global mechanism and the Young's modulus has a localised effect only. Furthermore, the yield stress of the weld metal is twice that of the parent metal due to which ratcheting occurs in the parent metal region within the ranges adopted for this study.

Variation of the plastic strain range with increasing E^{WM} is presented in Fig. 6. It is particularly interesting to note that the plastic strain range with and without mechanical load is almost the same for a particular cyclic thermal load. Fig. 7 presents the stress contours of the elastic analysis done on the welded pipe, with E^{WM} = 560 GPa, for a) only pressure load, b) only temperature load $\Delta\theta/\Delta\theta_o$=2 (100 °C) and $\Delta\theta/\Delta\theta_o$=4 (200 °C) and c) combination of both mechanical and temperature load. It is evident from them that the stress due to pressure alone re-distributes in the presence of the thermal stress causing the resultant stress to be similar to that of thermal stress alone. Thereby resulting in similar maximum plastic strain ranges values. Similar results were observed for all other values of E^{WM} undertaken in this study.

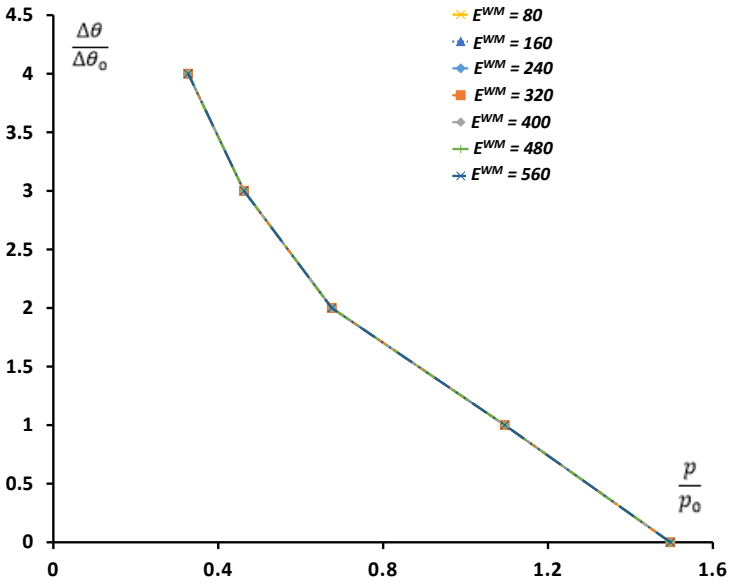

Fig. 5 Ratcheting curves of the welded pipe for varying Young's Modulus of weld metal

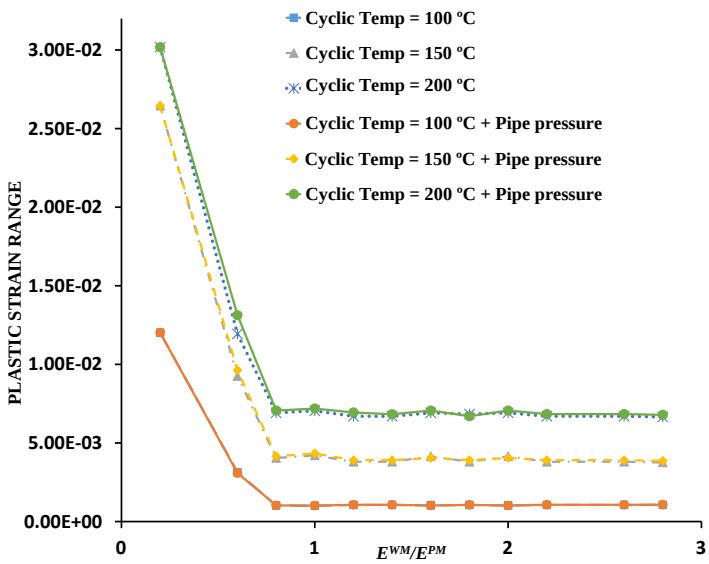

Fig. 6 Comparison of plastic strain range for varying Young's modulus of the weld metal, with and without mechanical load

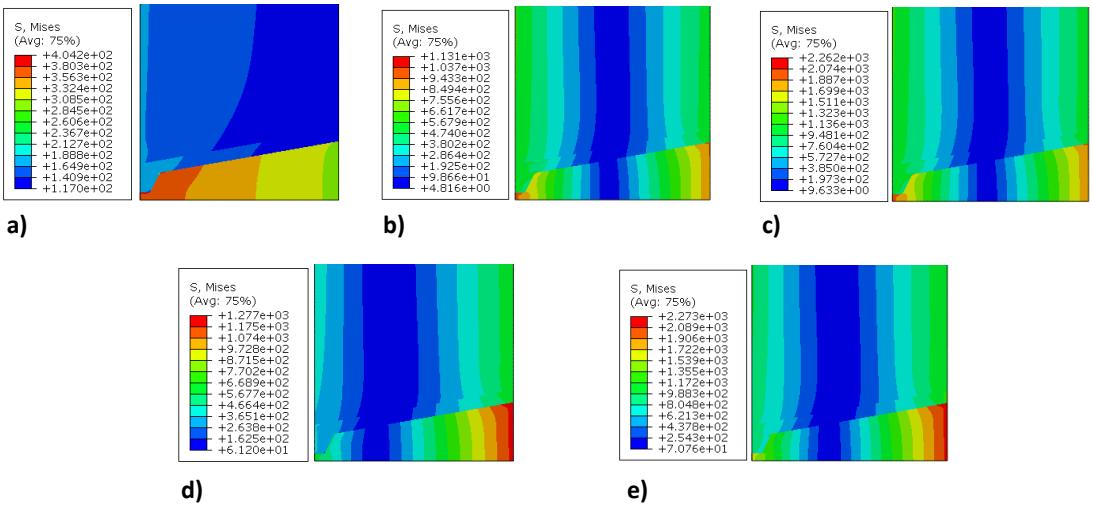

Fig. 7 Stress contours for elastic analysis; a) Due to internal pipe pressure; b) Due to cyclic temperature load, 100 °C; c) Due to cyclic temperature load, 200 °C; d) Due to combined load of internal pipe pressure and cyclic temperature load of 100 °C; e) Due to combined load of internal pipe pressure and cyclic temperature load of 200 °C

4.1.3 Effect of Yield Stress of weld metal, σ_y^{WM}

The yield stress of weld metal was varied from 115 to 460 MPa. Fig. 8 shows the ratchet limit interaction curves obtained.

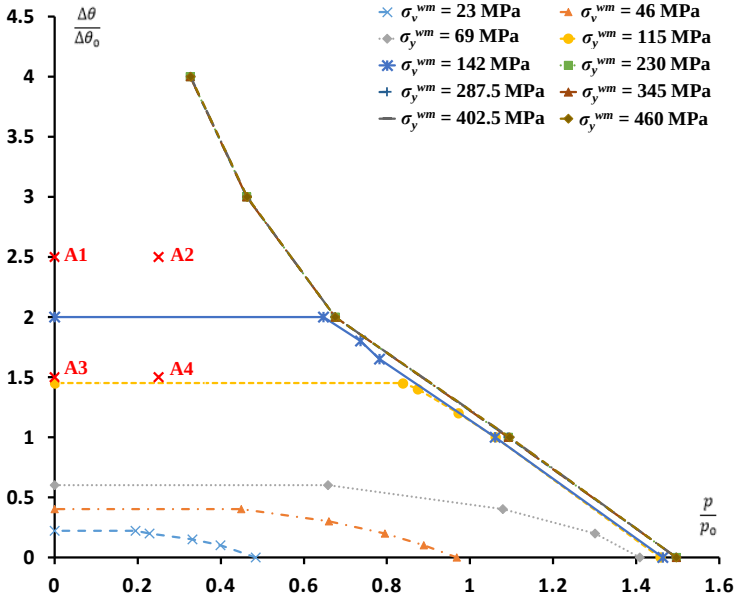

Fig. 8 Ratcheting curves of the welded pipe for varying yield stress of weld metal

When $\sigma_y^{WM} \big/ \sigma_y^{PM} \geq 1$, ratchet limit curves obtained are similar to Bree's like diagram and they superimpose each other. Ratcheting in these cases occurs in the parent metal. Analysis of limit load and ratchet limit curves at lower σ_y^{WM} values of 23, 46, and 69 MPa were done as special cases, represented in Fig. 8. When $\sigma_y^{WM} \big/ \sigma_y^{PM} \leq 1$, ratchet limit curve intersects the y-axis as the temperature is increased with ratcheting occurring in the weld metal region. The intersection of the

ratcheting curve on the y-axis indicates that the pipe experiences thermal ratcheting. At such low yield stress of the WM, the stress due to the thermal load, which is enhanced by the difference of the coefficient of thermal expansion of WM and HAZ and the stress due to the weld geometry is very high which may lead to ratcheting within the WM. In order to deeply understand the mechanism and validate the ratchet limit curves obtained from LMM, cyclic load conditions as indicated by the cyclic load points A1, A2, A3 and A4 in Fig. 8 and described in Table 3 are analysed by Abaqus step-by-step analysis. They are cyclic load points chosen with respect to σ_y^{WM} = 142 MPa. The results obtained are in agreement with the result from LMM analysis. The obtained histories of plastic strain magnitude, PEMAG, are given in Fig. 9. Cyclic load points, A1 and A2 which are above the ratchet limit curve predicted by LMM exhibit ratcheting behaviour while cyclic load points, A3 and A4 which are below the ratchet limit curve exhibit global shakedown behaviour. For load points A1 and A2, the strain increment is around 25-30% in 20 cycles (40 steps). While for A3 and A4 the strain rates stabilise indicating that they are under global shakedown. Thus we can confirm the ratcheting limit curves obtained by LMM.

Table 3 Cyclic load points analyzed using step by step analysis

Load Case	σ_y^{WM} (MPa)	p/p_o	$\Delta\theta/\Delta\theta_o$
A1	142	0	2.5
A2	142	0.2	2.5
A3	142	0	1.5
A4	142	0.2	1.5

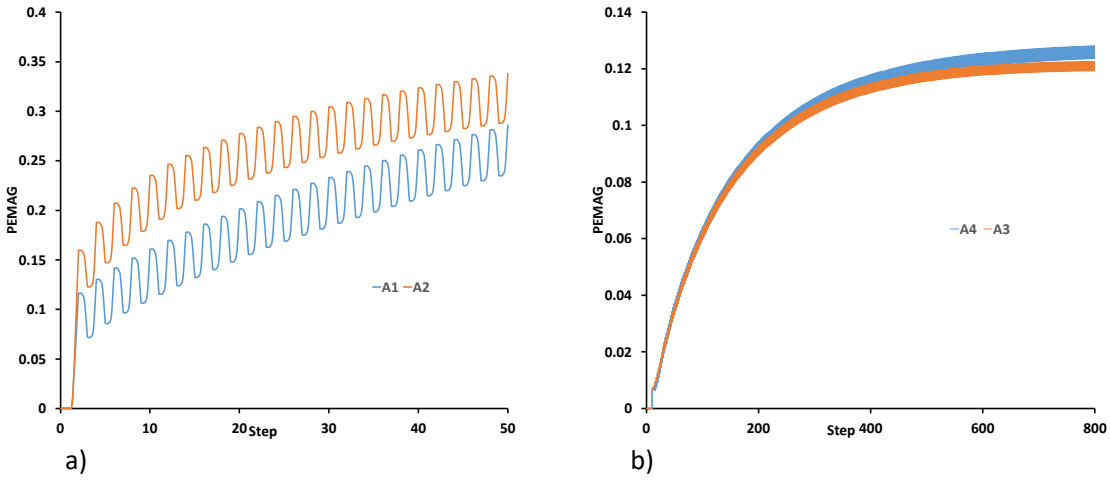

Fig. 9 History of plastic strain for the cyclic load point evaluated by step-by-step analysis a) for A1 and A2; b) A3 and A4

The limit load for $\sigma_y^{WM} / \sigma_y^{PM} \geq 1$ is constant. For σ_y^{WM} = 115MPa, only a slight reduction is observed in the limit load. This is because at limit load, all the different material zones reach their respective yield stress (Fig. 10(a)), which results in only a slight reduction of limit load. Whereas for lower σ_y^{WM} values of 23, 46, and 69 MPa, the limit load significantly reduces with stress concentration in the weld metal region and the maximum strain region occurring at the HAZ-WM metal interface.

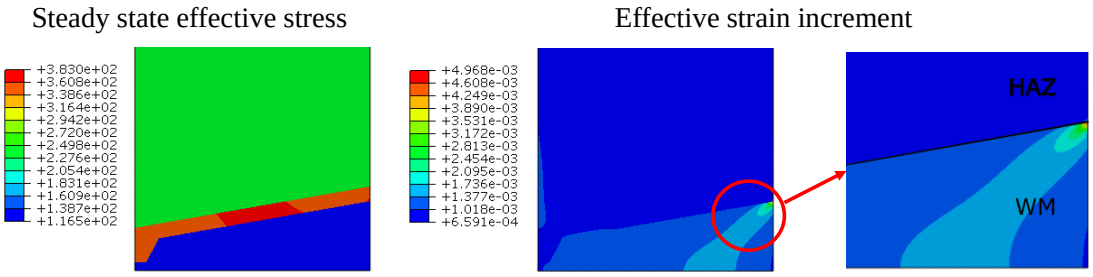

Fig. 10 a) At limit load, both the PM and WM have attained their respective yield stress for σ_y^{WM} = 115 MPa; b) The maximum strain region at limit load for σ_y^{WM} = 115 MPa

For $\sigma_y^{WM} / \sigma_y^{PM} \leq 1$, a strict Bree like diagram is not obtained and so the load points chosen for fatigue analysis differ from the ones mentioned in section 5. Fig. 11 indicates the shakedown and ratchet limit curve for σ_y^{WM} = 115 MPa and σ_y^{WM} = 142 MPa along with the load points analysed for fatigue study. Fig. 12 shows the variation of plastic strain range for $\sigma_y^{WM} / \sigma_y^{PM} \leq 1$, it is plotted with plastic strain range as the ordinate and $\Delta\theta/\Delta\theta_o$ as the abscissa. It is observed that for the particular cyclic load case analysed, the thermal load always dominates over the internal pressure load and the plastic strain range remains the same with or without the mechanical load. Also, the plastic strain range increases with an increase in the temperature.

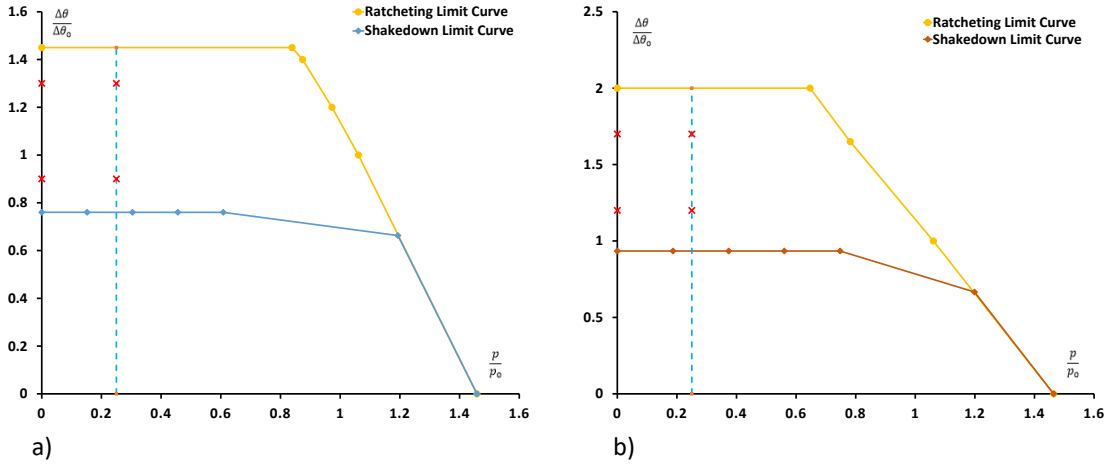

Fig. 11 Shakedown limit curve, ratchet limit curve and load points analyzed for fatigue study; a) For σ_y^{WM} = 115 MPa; b) For σ_y^{WM} = 142 MPa

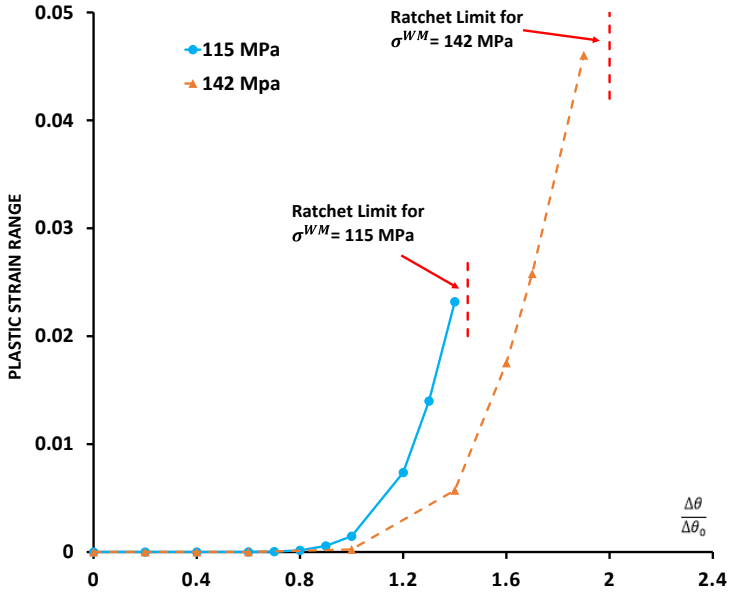

Fig. 12 Variation of plastic strain range for $\sigma_y^{WM} / \sigma_y^{PM} \leq 1$

Fig. 13 gives the variation of plastic strain range with increasing σ_y^{WM} for $\sigma_y^{WM} / \sigma_y^{PM} \geq 1$. It is interesting to note that for a defined cyclic temperature load the plastic strain range decreases to reach a minimum, after which it attains a constant value.

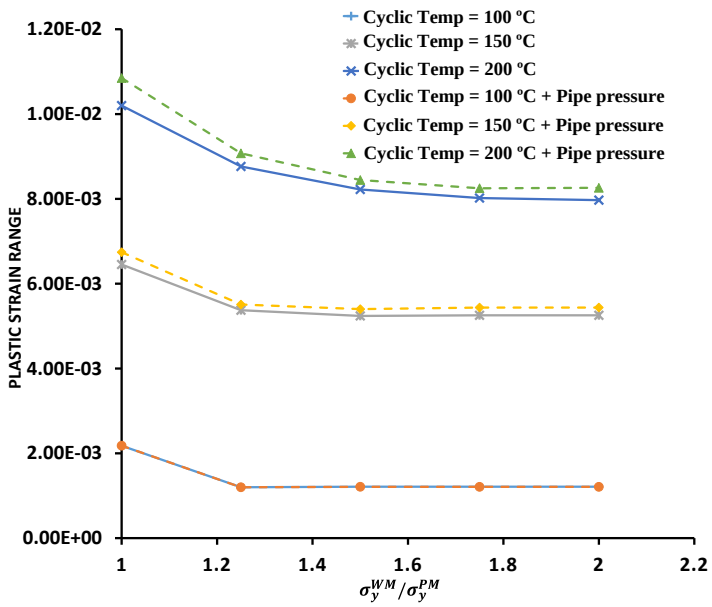

Fig. 13 Variation of plastic strain range for $\sigma_y^{WM}/\sigma_y^{PM} \geq 1$, with and without mechanical load

4.2 Influence of weld geometry

Five weld parameters b, c, e, α and β are individually varied to investigate the influence of weld geometry on ratcheting curve. They are varied as; b = 2, 3, 5(mm); c = 2, 3, 4(mm); e = 4.5, 6.5, 8.5(mm), α = 43, 53, 63 (°) and β = 8, 10, 16 (°). Fig. 14 shows the effect of the above parameters on the ratcheting limit, they do not influence the ratcheting curve. Hence it can be concluded that for the range considered in this study, the weld geometry does not affect the ratcheting curve.

Fig. 15 shows the variation of plastic strain range for different geometric parameters considered in this study. It can be seen that at lower temperatures the plastic strain range for all the parameters is similar, but as the temperature increases, there is an increase in the plastic strain range. The parameter, β causes the maximum variation in plastic strain range with an increase in temperature.

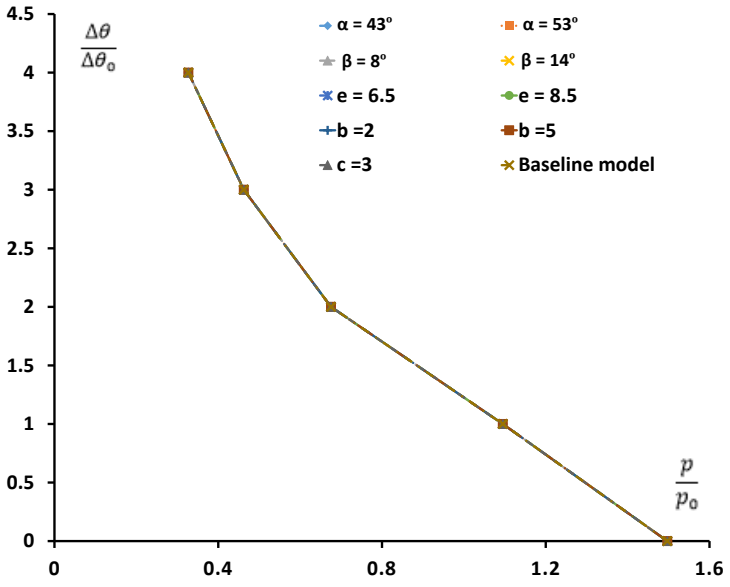

Fig. 14 Ratcheting curves of the welded pipe for varying geometric parameters

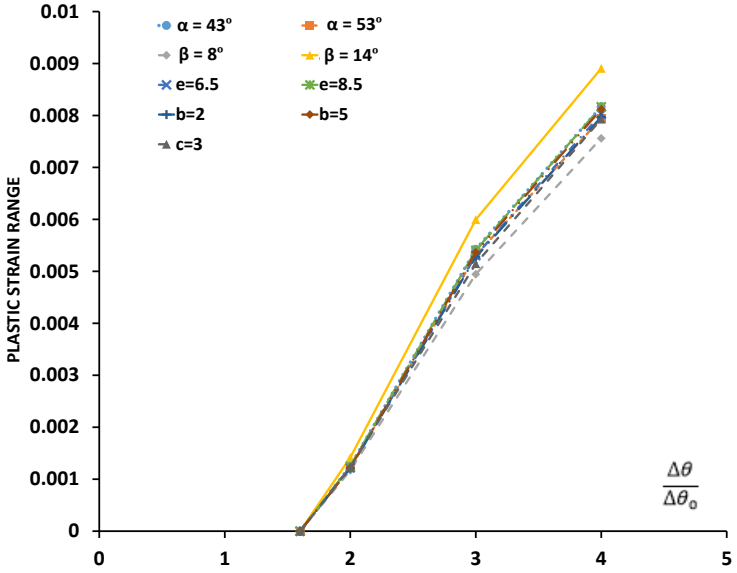

Fig. 15 Variation of plastic strain range for varying geometric parameters

4.3 Influence of ratio of inner radius to wall thickness

The effect of inner radius, R_i, to wall thickness, t, ratio (R_i/t) on the ratcheting limit is investigated in this sub-section. The inner radius is varied from 40 mm to 600 mm and the thickness of the pipe is maintained at a constant value of 40 mm. The ratcheting limit curves obtained are presented in Fig. 16.

For all R_i/t ratios, a typical Bree-like diagram is obtained. Increase in the R_i/t ratio decreases the limit load. This is because the increase in radii results in a larger area for pressure loading. The resultant high hoop and axial stresses leads to a reduced limit load and an overall movement of the ratchet limit curve towards the y-axis. It is also observed that the slope of the ratchet curve increases with an increase in the ratio of inner radius to wall thickness.

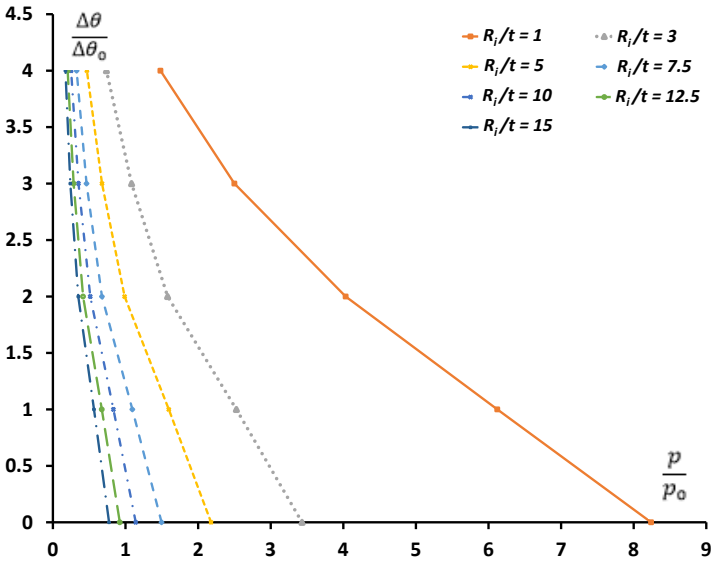

Fig. 16 Ratcheting curves of the welded pipe for varying R_i/t ratio, at constant t = 40 mm

Fig. 17, shows the effect of varying R_i/t on the plastic strain range for different cyclic temperature loads, with and without mechanical load. Compared to previous sections, fatigue analysis with mechanical load is done for $p/p_o = 0.1$. This is because $p/p_o = 0.25$ would limit the comparison studies as for $R_i/t \geq 10$, the body would exhibit ratcheting behaviour at higher temperatures as evident from Fig. 16. The variation of plastic strain range with and without mechanical load is minimal for a particular cyclic thermal load. This can be explained by the really high stress that is produced by the thermal shock occurring between the internal and external faces of the pipe. It can also be seen from Fig. 17 that for a given cyclic thermal load, plastic strain range decrease as we go from a thick pipe to a thin pipe configuration. This is because the thick pipe which has a smaller surface area experiences higher stress due to the cyclic temperature load compared to the thin pipes which result in lower plastic strain range.

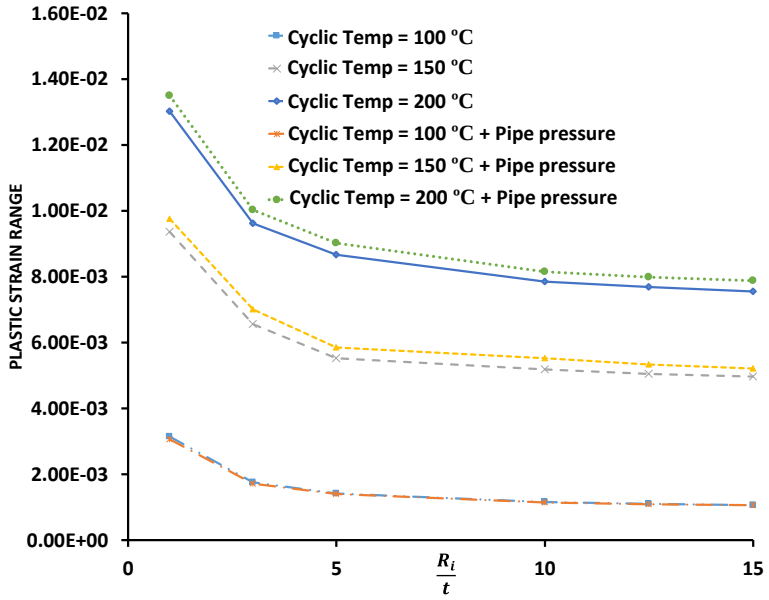

Fig. 17 Comparison of plastic strain range for varying R_i/t, with and without mechanical load

5 Further discussions

In the previous subsections, the results show how various material properties, weld geometry and ratio of inner radius to wall thickness affect the ratchet limit and the plastic strain range. Of which, R_i/t and σ_y^{WM} are the parameters that influence the ratchet limit curve and limit load the most. Whereas coefficient of thermal expansion, Young's modulus and weld geometry have minimal or no effect on the ratcheting limit curves for range considered in the study.

The limit loads obtained in Fig. 5 and Fig. 16 are normalised to the limit load of a pure PM pipe and replotted in Fig. 18. The trend line fitted to the data give the functions in equation 13 and 14.

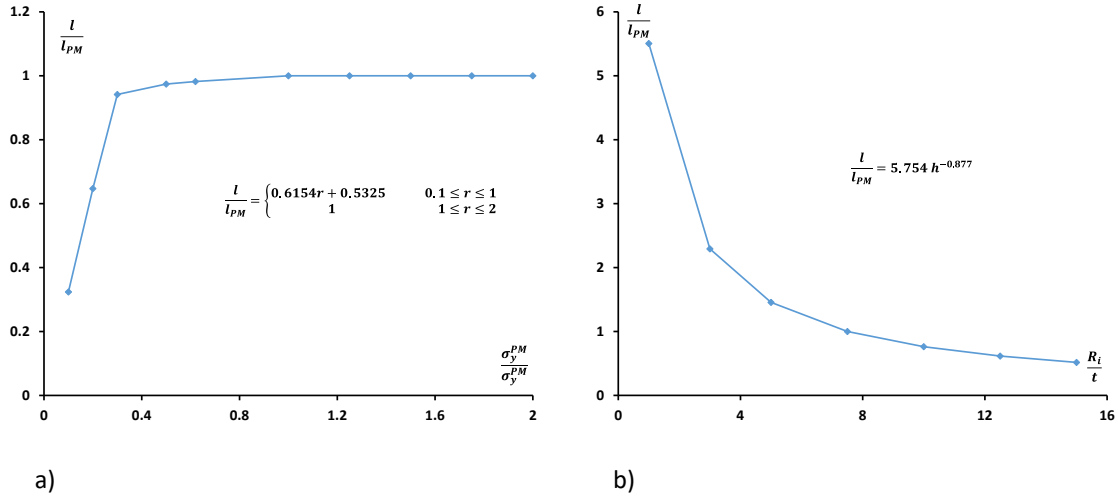

Fig. 18 (a) The effect of the yield stress of WM σ_y^{WM} on the limit loads (b) The effect of the ratio of inner radius to wall thickness R_i/t on the limit loads

$$\frac{l}{l_{PM}} = \begin{cases} 0.6154r + 0.5325 & 0.1 \le r \le 1 \\ 1 & 1 \le r \le 2 \end{cases} \tag{13}$$

$$\frac{l}{l_{PM}} = 5.754 h^{-0.877} \tag{14}$$

where l_{PM} is the limit load of a pure PM pipe, $r = \sigma_y^{WM} / \sigma_y^{PM}$ and $h=R_i/t$. Equation 14 is similar to the function obtained by Li et. al in [25] for a similar welded pipe.

For all the parametric study undertaken, the plastic strain range increases with an increase in the cyclic temperature load signifying a decrease in the low cycle fatigue life of the pipe. The most prominent area for LCF failure was the PM-HAZ interface for this case study and are shown in Fig. 19 (a) (highlighted by red circles and ordered for decreasing severity). All the critical locations are located at the interface between the PM and HAZ areas. Fig. 19 (b) represents the hysteresis loop with increasing cyclic thermal load for location 1. The mechanical load has minimal influence on the plastic strain range. This is because the stress produced by the thermal gradient due to the thermal shock is really high. Fig. 19 (c) represents the hysteresis loop with and without mechanical load for a cyclic thermal load of 150 °C. By analysing the shape and magnitude of the total strain range in location 1, a circumferential crack can be expected to start.

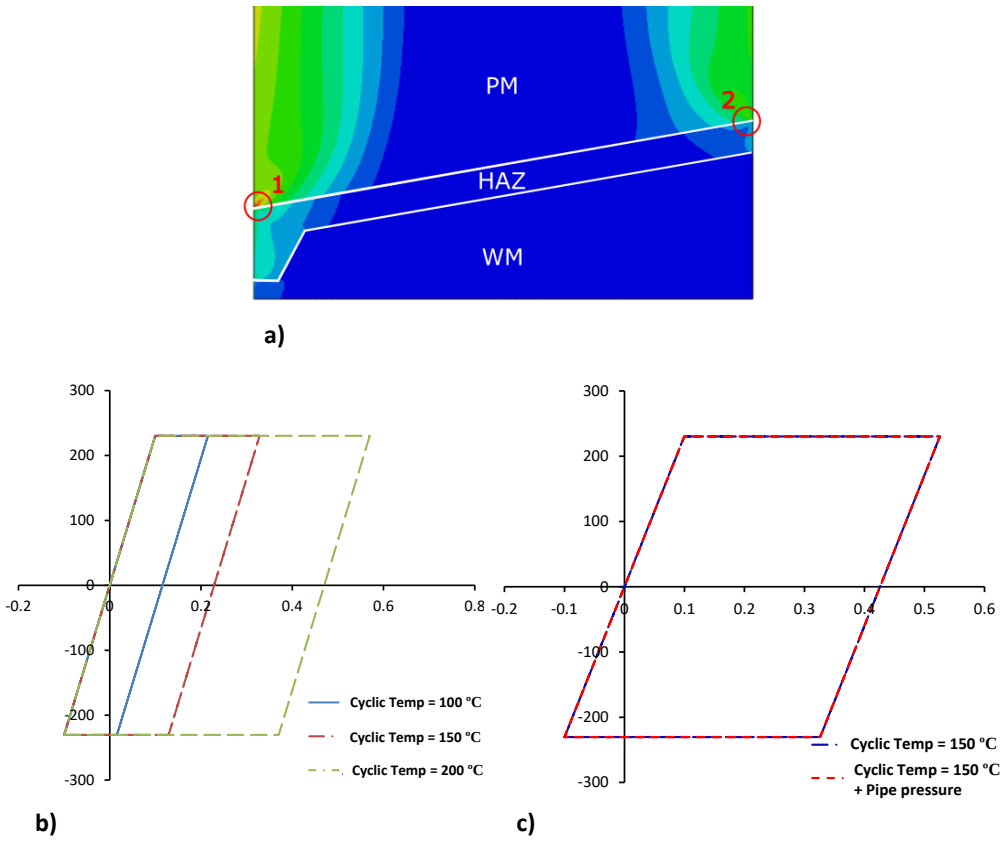

Fig. 19 (a) Critical location for LCF failure; (b) Hysteresis loop with increasing cyclic temperature load for location; (c) Hysteresis loop with and without mechanical load for a cyclic thermal load of 150 °C

6 Conclusions

The ratchet limit analysis and cyclic response assessment for a welded pipe subjected to a constant pressure and cyclic temperature under various conditions are studied using LMM. Weld geometry, pipe geometry and material parameters are varied to understand their influence. Based on the results obtained from this study, the following conclusions are drawn.

1. The coefficient of thermal expansion, Young's modulus and weld geometry have no effect on the ratcheting limit curves for the material properties and range considered in the study. They exhibit a Bree-like diagram.
2. For $\sigma_y^{WM} / \sigma_y^{PM} \geq 1$, a Bree like ratcheting limit curve is obtained with the failure mechanism occurring in the PM region. Though many factors such as ductility etc, influence the crack initiation region, based on the defamation analysis alone done in this study it is expected that the crack initiates at the HAZ-PM interface. For lower σ_y^{WM} analysed, ratcheting limit curve intersects the y-axis with an increase in temperature indicating that the secondary load is more prominent in causing failure within this range. The pipe experiences thermal ratcheting in the absence of pressure load.
3. An increase in the ratio of inner radius to pipe thickness decreases the limit load and reduces the ratchet limit.
4. The cyclic thermal load plays a crucial role compared to the internal pressure in determining the LCF life of the pipe undertaken in this case study as seen from the cyclic response

assessment work. The pipe pressure has minimum influence on the plastic strain range for varying Young's modulus, weld geometry, the yield stress of the weld metal and R_i/t ratio, for the range and loads considered in the study.

Acknowledgements

The authors gratefully acknowledge the support of the University of Strathclyde, the East China University of Science and Technology, and the 111 Project (B13020) during the course of this work.

References

[1] H. Chen, W. Chen, T. Li, and J. Ure, "On Shakedown, Ratchet and Limit Analyses of Defective Pipeline," *J. Press. Vessel Technol.*, vol. 134, no. 1, p. 11202, 2012.

[2] H. Chen and A. R. S. Ponter, "A Direct Method on the Evaluation of Ratchet Limit," *J. Press. Vessel Technol.*, vol. 132, no. 4, p. 41202, 2010.

[3] A. Sarkar, A. Nagesha, R. Sandhya, and M. D. Mathew, "Effect of temperature on ratcheting behaviour of 316LN SS," *Procedia Eng.*, vol. 55, pp. 650–654, 2013.

[4] A. Pal, R. Kumar, P. M. Dixit, and I. Sharma, "Ratcheting in cylindrical pipes due to an axially oscillating sharp temperature front," no. November, pp. 6–11, 2011.

[5] M. Ueda, T. Kano, A. Yoshitoshi, and T. Method, "Thermal Ratcheting Criteria and Behavior of Piping Elbows," vol. 1, no. February 1990, pp. 2–6, 2015.

[6] K. Zhang, "Characterization and Modeling of the Ratcheting Behavior of the Ferritic-Martensitic Steel P91," Karlsruher Institut für Technologie (KIT), 2017.

[7] H. Hübel, "Basic conditions for material and structural ratcheting," *Nucl. Eng. Des.*, vol. 162, no. 1, pp. 55–65, 1996.

[8] P. J. Amstrong and C. O. Frederick, "A mathematical represention of the multiaxial bauschinger effect," *CEGB Rep. No. RD / B /N 731*, no. September, pp. 1–24, 1966.

[9] J. L. Chaboche, "Continuous damage mechanics - A tool to describe phenomena before crack initiation," *Nucl. Eng. Des.*, vol. 64, no. 2, pp. 233–247, 1981.

[10] J. L. Chaboche, "Constitutive equations for cyclic plasticty and cyclic viscoplasticity," *Int. J. Plast.*, vol. 5, pp. 247–302, 1989.

[11] J. L. Chaboche, "On some modifications of kinematic hardening to improve the description of ratchetting effects," *Int. J. Plast.*, vol. 7, no. 7, pp. 661–678, 1991.

[12] T. Li, H. Chen, W. Chen, and J. Ure, "On the Ratchet Analysis of a Cracked Welded Pipe," *J. Press. Vessel Technol.*, vol. 134, no. 1, p. 11203, 2012.

[13] J. Abou-Hanna and T. E. McGreevy, "A simplified ratcheting limit method based on limit analysis using modified yield surface," *Int. J. Press. Vessel. Pip.*, vol. 88, no. 1, pp. 11–18, 2011.

[14] D. Mackenzie, J. T. Boyle, and R. Hamilton, "The elastic compensation method for limit and shakedown analysis: a review," *J. Strain Anal. Eng. Des.*, vol. 35, no. 3, pp. 171–188, 2000.

[15] R. Seshadri, "Inelastic evaluation of mechanical and structural components using the generalized local stress strain method of analysis," *Nucl. Eng. Des.*, vol. 153, no. 2–3, pp. 287–

303, 1995.

[16] W. T. Koiter, *General theorems for elastic-plastic solids*. North-Holland, 1960.

[17] C. E. Jaske, “Fatigue-Strength-Reduction Factors for Welds in Pressure Vessels and Piping,” *J. Press. Vessel Technol.*, vol. 122, no. August 2000, p. 297, 2000.

[18] J. Ure, H. Chen, and D. Tipping, “Calculation of a lower bound ratchet limit part 2 - Application to a pipe intersection with dissimilar material join,” *Eur. J. Mech. A/Solids*, vol. 37, pp. 369–378, 2013.

[19] H. Chen and A. R. S. Ponter, “A method for the evaluation of a ratchet limit and the amplitude of plastic strain for bodies subjected to cyclic loading,” *Eur. J. Mech. A/Solids*, vol. 20, no. 4, pp. 555–571, 2001.

[20] H. Chen and A. R. S. Ponter, “Linear matching method on the evaluation of plastic and creep behaviours for bodies subjected to cyclic thermal and mechanical loading,” *Int. J. Numer. Methods Eng.*, vol. 68, no. 1, pp. 13–32, 2006.

[21] A. R. S. Ponter and H. Chen, “A minimum theorem for cyclic load in excess of shakedown, with application to the evaluation of a ratchet limit,” *Eur. J. Mech. A/Solids*, vol. 20, no. 4, pp. 539–553, 2001.

[22] J. Ure, H. Chen, and D. Tipping, “Verification of the Linear Matching Method for Limit and Shakedown Analysis by Comparison With Experiments,” *Vol. 1A Codes Stand.*, p. V01AT01A036, 2013.

[23] P. C. Lam and J. S. Gail, “Experimental Studies of Ratcheting of Pressurized Pipe,” no. May, 1991.

[24] B. Brickstad and B. L. Josefson, “A parametric study of residual stresses in multi-pass butt-welded stainless steel pipes,” *Int. J. Press. Vessel. Pip.*, vol. 75, no. 1, pp. 11–25, 1998.

[25] T. Li, H. Chen, W. Chen, and J. Ure, “On the shakedown analysis of welded pipes,” *Int. J. Press. Vessel. Pip.*, vol. 88, no. 8–9, pp. 301–310, 2011.